Zeitschrift für Geomorphologie, Vol. 61 (2017), Suppl. 2, 179–197 **Article**
published online May 2017; published in print November 2017

The contribution of geomorphometry to the seabed characterization of tidal inlets (Wadden Sea, Germany)

F. Mascioli, G. Bremm, P. Bruckert, R. Tants, H. Dirks and A. Wurpts

with 10 figures and 2 tables

Abstract. The monitoring policies of subtidal marine areas, as regulated by the FFH and MSFD, require stable measures and objective interpretation methods to ensure accurate and repeatable results. The nature of Wadden Sea inlets seabed have been investigated trough the analysis of bathymetrical and backscatter data, collected simultaneously by means of high-resolution multibeam echosounder, in conjunction with validation samples. The datasets allowed a robust approach to characterize substrate and bedforms, using objective and repeatable methods. The geomorphometric approach gives a substantial contribution to extract quantitative information on morphology and bedforms from bathymetry. DEMs of four tidal inlets have been used to calculate morphometric parameters, compare the inlets morphology and provide a classification of slope and profile curvature. Classified morphometric parameters have been applied to a detailed characterization of Otzumer Balje seabed. Very steep slopes and breaks of slope potentially related to substrate variations have been mapped and statistically investigated with respect to their depth distribution and spatial orientation. The computation of multiscale Benthic Position Index identified morphological features and bedforms at broad and fine scales. The geological and geomorphological meaning of morphometric parameters were extracted by means of quantitative comparison with backscatter intensity and samples. Backscatter was processed for radiometric corrections, geometrical corrections and mosaicking, to get intensities representative of the substrate characteristics. Within this integrated approach, it was possible to quantitatively analyse the complex morphology of subtidal areas of the Wadden Sea tidal inlets. At detailed resolution, the integration of bathymetric and backscatter data provided a bedforms and substrate characterization according to the main habitat classification schemes.

Keywords: seabed mapping, tidal inlet, geomorphometry, backscatter, swath bathymetrical systems, Wadden Sea, Germany

1 *Introduction*

The Wadden Sea is located along the southern North Sea, stretching for almost 500 km between Den Helder (Netherlands) and Skallingen (Denmark). It covers an area of nearly 3,300 km^2 and is one of the world's largest intertidal systems encompassing a multitude of transitional zones between land, marine and estuaries environments (Dittmann 1999, Dankers et al., 2012). Several coastal infrastructures, a dense network of submarine energetic utilities, as well as dredging, dumping and fishing activities, strongly interact with the natural environment (Dissanayake et al. 2012, Wang et al. 2012). Since 2009 it is an UNESCO World Heritage site and is protected in framework of the Trilateral Wadden Sea Plan entailing policies, measures, projects and actions agreed upon by The Netherlands, Germany and Denmark.

The high natural heritage and the intense human activity require an increasing knowledge of the subtidal environment. The Marine Strategy Framework Directive 2008/56/EEC and the Council Directive 92/43/EEC on the conservation of natural habitats formally provide moni-

DOI: 10.1127/zfg_suppl/2017/0354 0372-8854/17/0354 $ 15.25

toring requirements and basic guidelines, including morphology and substrate composition within the ecological quality elements to be periodically monitored. Establishing that monitoring has to outline the environmental changes due to the human activities, the EU Directives in fact require filtering instrumental effects, natural variables and human subjectivity out of the acquisition and interpretation processes.

The use of acoustic remote-sensing, in conjunction with ground-truth validation samples, provides a robust approach to characterize marine substrate and bedforms (Miccadei et al. 2011, 2012, Micallef et al. 2012). Recent technological advancements of swath bathymetric systems, as multibeam echosounders and phase measuring bathymetry systems, drastically improve the effectiveness of hydroacoustics, as they collect high-resolution bathymetry and high-quality backscatter intensities at the same time (Les Bas & Huvenne 2009, Bartholomä et al. 2011).

The interpretation of DEMs and backscatter mosaicked imageries has been conventionally done by manual experts analysis, whereby expert analysis divides bathymetry and backscatter into regions of similar attributes, linked to geological and geomorphological features by means of ground-truthing samples. As this procedure is affected by high subjectivity, the research of repeatable approaches became of primary importance (Brown et al. 2011, Diesing et al. 2014, Ismail et al. 2015). Geomorphometry gives a substantial contribution to the objective and quantitative analysis of bathymetry. Several studies prove its potential to help the scientific community and governmental agencies advance their understanding of seabed geology, geomorphological processes and habitats (Iampietro et al. 2005, Wilson et al. 2007, Lecours et al. 2015). Even though it has been successfully applied to a variety of subaerial environments (Jasiewicz et al. 2015 and references in), it still has a number of characteristics that make problematic the application of traditional geomorphometric techniques to the submarine landscape (Lecours et al. 2015). The low availability of data, usually with different resolution, and a more smooth morphology makes the computation of morphometric parameters hard (Micallef et al. 2007). The difficulty to achieve a representative ground-truthing is a strong limitation to the results calibration, even more in such areas where water turbidity drastically reduces the direct observation of seabed by means of optical methods as cameras.

The aim of this paper is a methodological contribution to extract geological and geomorphological characteristics of seabed from hydroacoustic data and samples, integrating geomorphometric and backscatter analysis. It provides new quantitative information on the tidal inlets morphology through the computation of morphometric parameters and proposes a multiscale morphological classification to identify bedforms. The comparison of morphometric parameters, backscatter intensities and samples allowed the seabed characterization, outlying the relations between bedforms, seabed composition and geomorphological process. Each of the performed analysis gives important information to characterize the seabed and are valuable inputs for environmental mapping, monitoring purposes and consistent to the main habitat classification schemes.

2 *Study area*

The present study focuses on the subtidal areas of the south-west German Wadden Sea, extended from the Dutch border, in the west, to the estuary of river Elbe, in the east (Fig. 1). The Wadden Sea is a meso-tidal environment, with semi-diurnal tides. It is separate from the North Sea by the Frisian barrier islands, resulting from coastal depositional processes occurred during the Late-Holocene sea-level high-stand (Lüders 1953). Several tidal inlets cross the barrier islands and connect the tidal basins to the North Sea trough a system of channels, flood delta and ebb delta (Hayes 1980). The maximum depth is about –25 m, generally observed along the main tidal channels.

The stratigraphic setting is given by a Holocene wedge-like depositional body, lying on top of the Upper Pleistocene succession made of alternating sandy and organic clayey layers (Streif 1998, 2004). The Holocene succession consists of a basal organic sequence made of peat and clay, covered by fine-grained sandy, silty and clayey deposits, with intercalated semi-terrestrial peat layers (Zeiler et al. 2000, Chang et al. 2006, Bungenstock & Weerts 2012). The average thickness of the Holocene succession ranges from 10 to 12 m, wedging out against the Pleistocene hinterland. Seaward, it ends at a steep slope to a water depth of about –25 m (Zeiler et al. 2000).

Surficial sediments are mainly made of fine to coarse sands, with variable mud fraction. Locally muddy deposits are present, made of physically or biodeposited muds (Ragutzki 1980, Flemming & Davis 1994, Zeiler et al. 2008, Bartholomä et al. 2011). Surficial sediments are permanently reworked and mobilized by waves- and tidal-induced currents, with a continu-

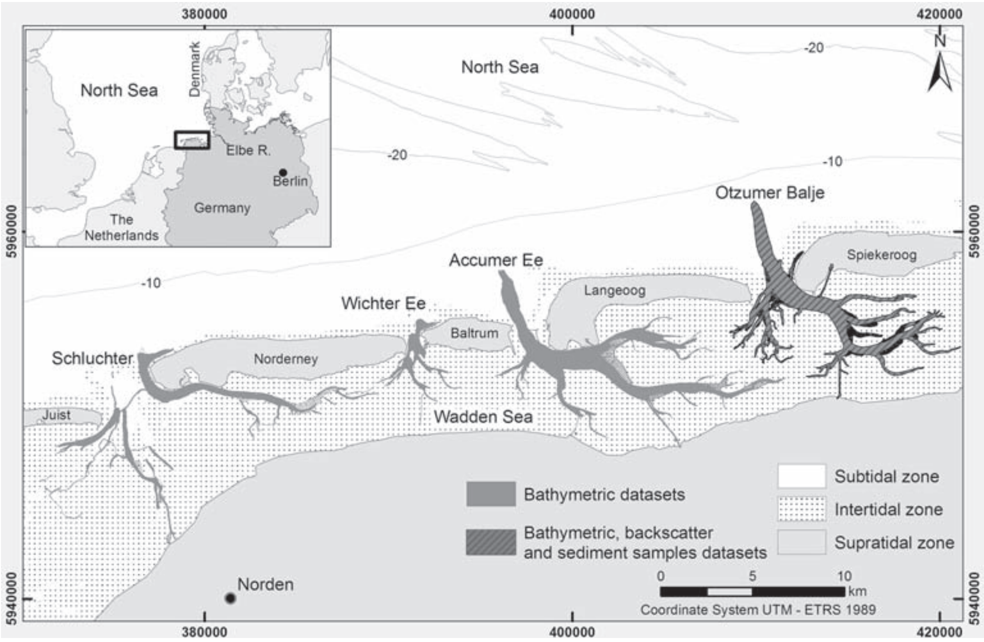

Fig. 1. Location of the study area and the four analysed tidal inlets. Grey areas indicate the extension and the type of used datasets.

ous exchange of sediments between flood deltas, channels and ebb deltas (Ladage et al. 2006, Son et al. 2011). The sediment mobilization induces very intense morphodynamics in the inlets (Meyer et al. 2014), producing bedforms mainly made of small to large sand waves (Ernstsen et al. 2005).

3 *Methods*

3.1 *Data set information*

The study is based on three datasets acquired between 2012 and 2014 (Fig. 2). The first one is the full-coverage swath bathymetry of Schluchter (2012), Wichter Ee (2013), Accumer Ee (2013) and Otzumer Balje (2014) inlets. The total covered area is ca. 55 km^2, with water depth from –1.5 m up to –25 m (Fig. 1). The second dataset consists on the full-coverage backscatter intensities only for Otzumer Balje, collected simultaneously to the bathymetrical data (2014). It covers an area of about 19 km^2. Both bathymetric and backscatter datasets are collected by the R/V Nynorderoog by means of hull-mounted Kongsberg EM3002 D multibeam echosounder, operating at a frequency of 300 kHz and fully compensating for vessel motion. Sound velocity profiles were measured every 2 hours, to account for the hydrology effects. Position and elevation were provided by RTK-Fixed DGNSS system with correction data supplied by the German satellite positioning service SAPOS®. Bathymetric raw data were processed with QPS QINSy software by accounting for sound velocity variations, tides and basic quality control. Digital Elevation

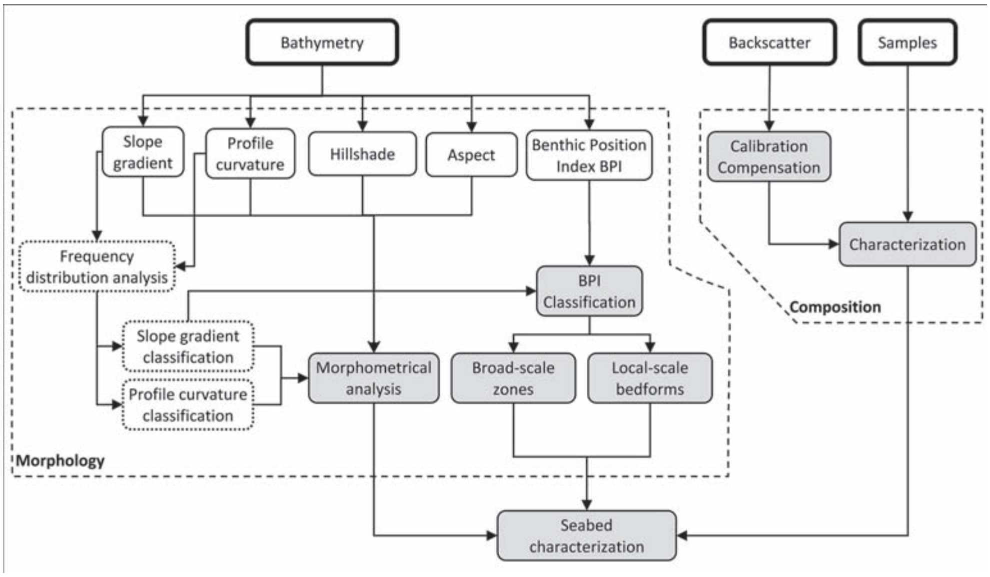

Fig. 2. Workflow of the applied methodology, showing the datasets (thick-bounded cells), the computed morphometric parameters (white cells), the approach performed on 4 inlets aimed to classify the morphometric parameters (dashed-bounded cells) and the analysis performed on Otzumer Balje aimed to the seabed characterization (grey cells).

Models (DEMs) were realized with a cell size of 1 m. Raw backscatter was processed with QPS Fledermaus GeoToolbox software for radiometric corrections, geometric corrections and mosaicking (Beaudoin et al. 2002, Fonseca & Calder 2006). Backscatter mosaic was exported as raster with a cell size of 1 m.

The third dataset consists on over 120 sediment samples from Otzumer Balje, collected in 2014 and 2015 to ground-truth backscatter intensities, with a 50 litre Van Veen grab by means of the R/V Burchana. The number and position of samples were planned based on a preliminary interpretation of bathymetry and backscatter. The samples analysis was performed through qualitative observations and grain-size analysis by sieving.

3.2 *Morphometric parameters classification*

Hillshade, slope and profile curvature were derived from the DEMs of four inlets (Fig. 2), using the Geographic Information System ArcGIS^{TM} 10.3, on a 3 × 3 cell neighbourhood around the centre cell. Hillshade was used to enhance the visualization of raster surfaces. The frequency distribution of slope and profile curvature was statistically investigated, to compare the morphology of the inlets. Slope and profile curvature have been then classified using the Jenks' Natural Breaks clustering algorithm, selecting breaks minimizing the variance within a class and maximizing the variance between classes (Jenks & Caspall 1971). The classification identified 5 classes of slope and 5 classes of profile curvature for each inlet. The mean of each class breaks were calculated to compute unique break values over the inlets.

3.3 *Seabed characterization*

3.3.1 *Geomorphometric analysis*

The mean values of the class breaks were used to perform the geomorphometric analysis of Otzumer Balje (Fig. 2). Slope classes were used to identify steep and very steep slopes. Profile curvature classes were used to map convex breaks of slope. Then they were filtered by a neighbourhood filter on 20 × 20 m squared zones, to outline areas where steep or very steep surfaces coexist with convex breaks of slope. The depth distribution and orientation of resulting surfaces have been statistically analysed by the comparison with bathymetry and aspect raster surfaces.

A multiscale terrain classification has been performed trough the computation of the Benthic Position Index BPI (Erdey-Heydorn 2008). The BPI is the marine version of the Topographic Position Index TPI introduced by Weiss (2001), and has been applied to several marine studies in recent years (Iampietro et al. 2005, Lundbald et al. 2006, Wilson et al. 2007, Diesing et al. 2009). It consists on a focal statistical analysis evaluating the depth difference between a cell depth and the mean depth of the surrounding cells, within an user defined neighbourhood geometry (Evans et al. 2006). The result is an indication of whether any particular pixel is part of a positive (e.g. crest) or negative (e.g. valley) feature of the surrounding terrain (Wilson et al. 2007). The scale of the BPI calculation is denoted by the scalefactor, defined as the neighbourhood size multiplied by bathymetric data resolution, and strongly influences the results: smaller scalefactors better represent small features (Lundbald et al. 2006, De Reu et al. 2013). Our calculations were performed using an annulus neighbourhood shape (Lundbald et al. 2006)

Table 1. Classified slope positions and classification criteria.

Broad-Scale BPI (scalefactor 200)		Fine-Scale BPI (scalefactor 20)	
Slope position classification	BPI and slope criteria	Slope position classification	BPI and slope criteria
Depressions	BPI ≤ –1 SD	Depressions	BPI ≤ –0,1 SD
Slopes	–1 SD < BPI ≤ 1 SD Slope > 2°	Deeply incised depressions	BPI ≤ –1 SD
Reliefs	BPI > 1 SD	Slopes	–0,1 SD < BPI ≤ 0,1 SD Slope > 2°
Flats	–1 SD < BPI ≤ 1 SD Slope < 2°	Ridges	BPI ≥ 1 SD
		Local ridges	BPI > 0,1 SD
		Flats	–0,1 SD < BPI ≤ 0,1 SD Slope < 2°

by means of the GIS implementation Topography Tools for ArcGIS™ 10.3 (Jenness 2006). The neighbourhood sizes were chosen based on an examination of the bathymetry prior to the BPI calculation, which showed large features size about 300 meters across (e.g. tidal channel) and small bedforms average size about 20 m across (e.g. sand waves). The BPI was, therefore, computed at two different scales: a broad-scale, with inner-radius = 20 m and outer-radius = 200 m, and a fine-scale, with inner-radius = 5 m and outer-radius = 20 m. BPI grids were standardised by subtracting the mean BPI from each BPI data point value and dividing by the standard deviation. In this way, the mean BPI had a value of 0 and the standard deviation had a value of –1/+1 (Wilson et al. 2007). The broad-scale BPI was classified into 4 slope positions and the fine-scale BPI into 6 slope positions (Table 1). The classifications are based on the standard deviation from the depth, which take into account the variability of depth values within the neighbourhood (Evans et al. 2016, Lundbald et al. 2006, Weiss 2001).

At broad-scale, thresholds values as proposed by Weiss (2001) were applied. Thresholds values of the fine-scale classification were set as reported in Table 1, in order to adjust them to the relatively smoothed morphology of minor bedforms. The critical slope value discerning slopes and flats was set based on the results of the slope classification performed over four inlets (Table 1).

3.3.2 *Backscatter analysis*

The geomorphometric results were compared with substrate characteristics, derived from the backscatter intensity as defined by the sonar equation

$$EL = SL - 2TL + BS + 10 \log A,$$

where EL is the echo level recorded by the sonar, SL is the source level, TL is the energy loss in the water column, BS is the backscatter strength depending on the seabed type, and A is the instant ensonified area (Lurton 2002).

The recorded echo was processed to be rid of those parts of the signal that are not directly related to the seabed type itself, as water column effects and morphology, and access the backscatter information intrinsic to the bottom composition, since the bathymetry provided by the sonar allows the computation of all the variables of the equation. The processing chain started with the calibration of the signal levels emitted and received by the sensor. The next stages were data corrections, required for qualitative and quantitative backscatter estimation and exploitation. They included i) the compensation of the instant ensonified area as a function of the sonar characteristics and the incident angle between the acoustic waves and the seabed, ii) the compensation of transmission loss as a function of the transducer-seafloor distance and the absorption coefficient of the water, iii) the correction of BS for the incident angular dependency. The last step was the mosaicking, providing backscatter intensities directly depending on the substrate composition (Augustin & Lurton 2005, Lamarche et al. 2011, Lurton & Lamarche 2015 and references in). The different acoustic facies of the mosaic were then linked to the sediment types by means of ground-truth samples (Fig. 2).

Information on morphology and seabed composition were combined in a single map, which was slightly smoothed to eliminate small and isolated areas with high uncertainty and that were probably misclassified (Micallef et al. 2012). In this way, each cell of the produced map was classified in terms of morphology, composition and geomorphologic information.

4 *Results*

4.1 *Slope and profile curvature classification*

Slope and profile curvature over the four inlets were statistically investigated in terms of frequency distribution and results were plotted as cumulative curves (Fig. 3). Slope frequency has a similar unimodal distribution over the inlets, with over 85 % of the surveyed area having slope < 5° and about 60 % with slope < 2°. Steepest surfaces with slopes > 20° characterize about 1 % of the whole area.

The profile curvature has a unimodal and slight positive skewed distribution, with positive and negative values describing concave and convex surfaces, respectively (Fig. 3). The maximum frequency is between 0 m^{-1} to –2 m^{-1}. For each inlet, over 90 % of the surveyed area has

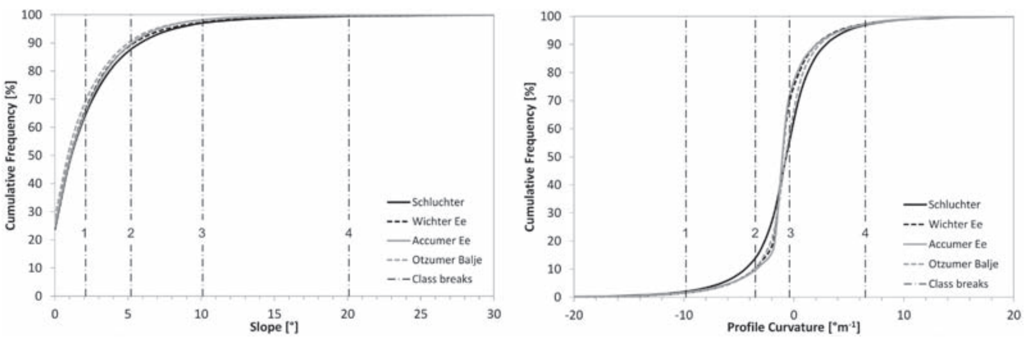

Fig. 3. Cumulative frequency distribution of slope and profile curvature of four inlets. Positive and negative values of profile curvature describe concave and convex surfaces, respectively. Mean class breaks 1 to 4 refer to the Fig. 4.

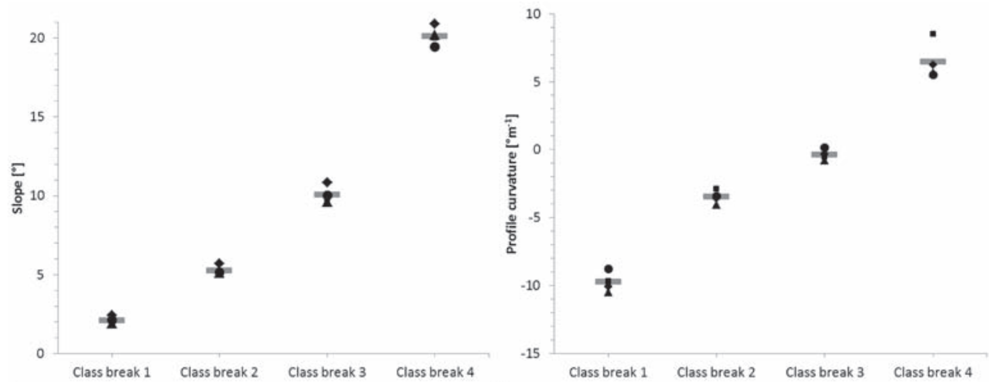

	1	2	3	4
◆ Schluchter	2,4	5,7	10,9	20,9
● Wichter Ee	2,1	5,2	10,0	19,4
▲ Accumer Ee	1,9	5,1	9,6	20,2
■ Otzumer Balje	1,9	5,0	9,7	20,0
— Mean	2,1	5,2	10,1	20,1

	1	2	3	4
◆ Schluchter	-10,1	-3,6	-0,3	6,2
● Wichter Ee	-8,8	-3,4	0,2	5,5
▲ Accumer Ee	-10,5	-4,0	-0,8	5,7
■ Otzumer Balje	-9,7	-2,9	-0,6	8,5
— Mean	-9,8	-3,5	-0,4	6,5

Fig. 4. Class breaks of slope (left) and profile curvature (right) of each inlets, computed using the Jenk's Natural Breaks algorithm. Grey dashes are the mean value of each break over the four inlets.

Table 2. Generalized classes of slope and profile curvature based on the mean value of classes breaks of each inlet.

Slope		Profile Curvature	
Flat	$S < 2°$	Very convex	$C < -10°m^{-1}$
Gently sloping	$2° < S < 5°$	Convex	$-10°m^{-1} < C < -4°m^{-1}$
Sloping	$5° < S < 10°$	Slightly convex	$-4°m^{-1} < C < 0°m^{-1}$
Steep	$10° < S < 20°$	Slightly concave	$-0°m^{-1} < C < 7°m^{-1}$
Very steep	$> 20°$	Concave	$> 7°m^{-1}$

a profile curvature between $-4\,m^{-1}$ to $7°m^{-1}$, about 75 % has negative values. 2 % of the surface contains the highest absolute values, with curvature $< -10\,m^{-1}$ and $> 7\,m^{-1}$.

The classification of slope and profile curvature by means of the Jenk's Natural Breaks algorithm identifies four main class breaks for each inlet (Fig. 4).

Since resulting values of class breaks over the four inlets are similar, mean values were computed and used for a generalized classification of slope and profile curvature (Table 2).

4.2 *Seabed characterization of Otzumer Balje*

4.2.1 *Geomorphometric characterization*

The broad-scale BPI computed on Otzumer Balje identifies wide flat surfaces with slope values < 2°. They mainly cover areas shallower than −5 m and are referable to the tidal flat (Fig. 5a).

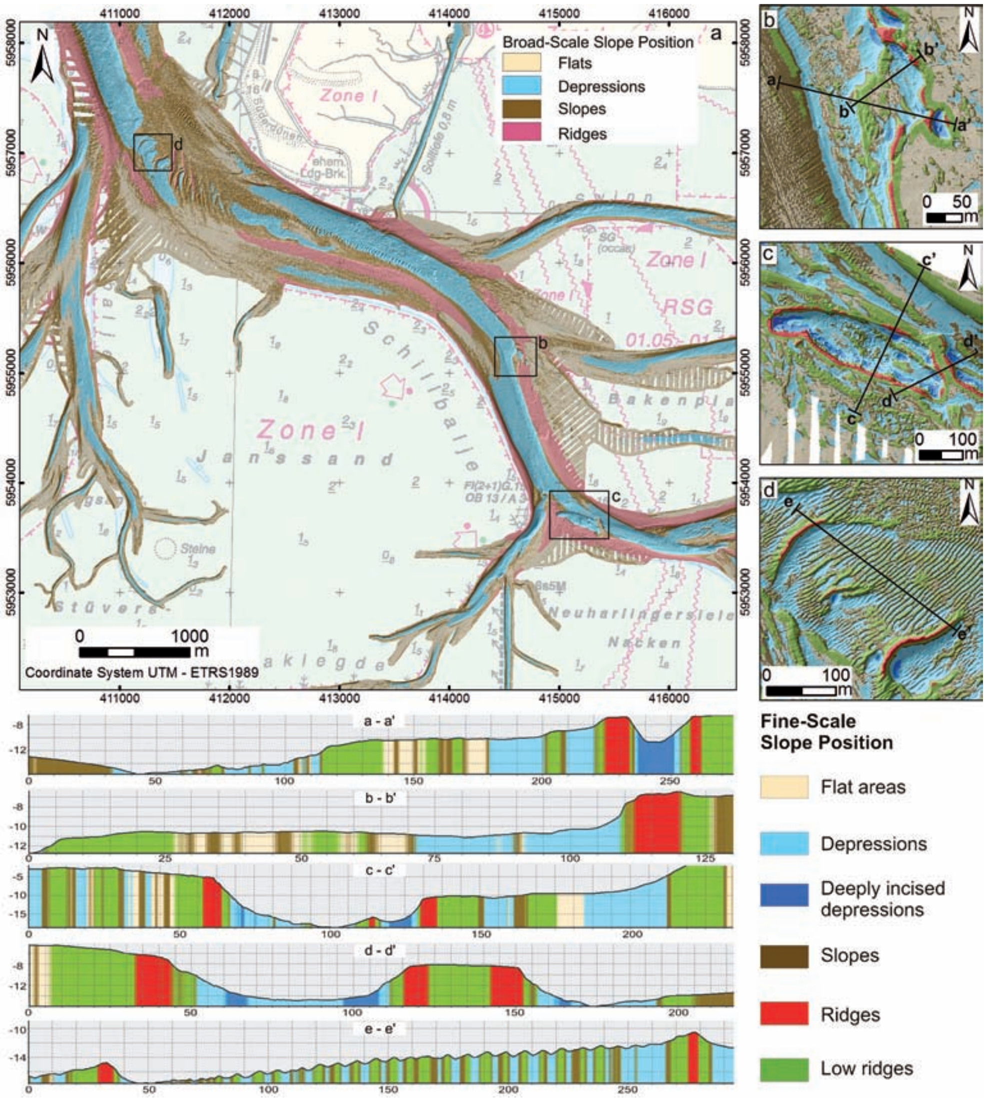

Fig. 5. Morphological classification based on the Benthic Position Index, computed at broad-scale and fine-scale (units are meters).

Flats are crossed by depressions consisting on the tidal-channels, characterized by flat or u-shaped bottoms (Fig. 5a). The fine-scale BPI identifies deeply incised sub-circular depressions, located on the margin of the main channel (Fig. 5b, c). They are 5 to 6 m deep, bounded by convex breaks of slope and very steep slopes (Fig. 6a, b).

Slopes identify steeping zones connecting depressions and shallow flats, as well as the flanks of the largest sand waves (Fig. 5a). The slopes of tidal channels have gradients between 10° and 20°. Locally, the alternation of very steep surfaces ($S > 20°$) and gently sloping ($2° < S < 5°$) or flat ones ($S < 2°$) results into a terraced morphology of the channel profile (Fig. 6a).

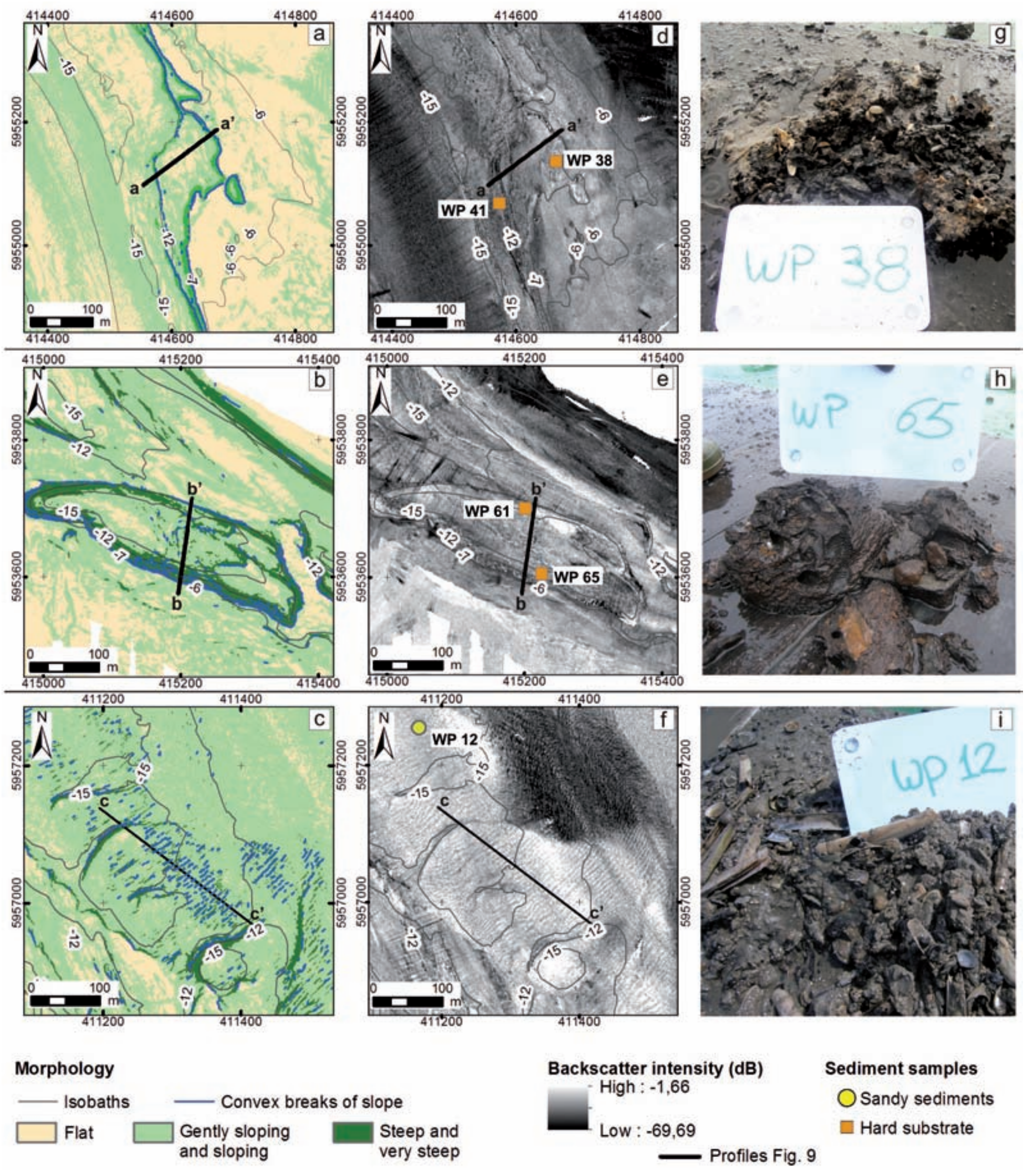

Fig. 6. Geomorphometric mapping, backscatter intensities and samples of the fine-scaled bedforms. a, b: Two orders of scarps identified by convex breaks of slope, steep and very steep slopes, located between −7 and −12 m. c: Sand waves characterized by steep and very steep slopes and convex morphology of the crests. d, e: Backscatter intensity showing high values on flat and gently sloping areas, and low values on steepest surfaces. f: Backscatter intensity with relative high values, showing a pattern consistent with the morphology of small and medium sand waves. g, h: Peat fragments collected on the very steep slopes. i: sandy sediments with a coarse fraction made of shells, collected on sand waves.

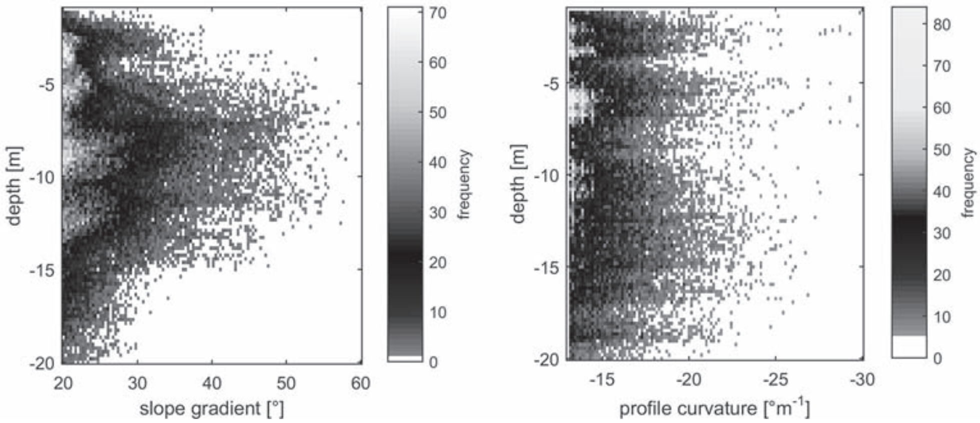

Fig. 7. Depth distribution of very steep slopes (S > 20°) and convex breaks of slope (C < $-10°m^{-1}$).

Ridges identify the crests of large sand waves as well as the convex edges connecting slopes and flats (Fig. 5a). At fine-scale, ridges identify the boundaries of the deeply incised depressions and high-morphological structures along the main channel (Fig. 5b, c) as well as the crests of large sand waves located on the channel bottom (Fig. 5d). The low ridges class identifies the crests of small and medium sand waves, as well as moderate elevations within flats and u-shaped depressions (Fig. 5,b, c, d). All the ridges are characterized by convex breaks of slope, which outline sharp transitions from flats to slopes (Fig. 6a, b, c), as well as the crests of the sand waves (Fig. 6c). The flank of large sand waves are characterized by very steep slopes (S > 20°), whereas medium and small ones mainly have steep flanks (Fig. 6).

The analysis of the depth distribution of very steep surfaces (> 20°) shows that they are mainly located at four bathymetric levels (Fig. 7). The first level has a depth of about –3 m. It is characterized by a high concentration of surfaces with slope up to 22° and maximal values of about 35°. The second level is located between –5 m to –6 m, and presents a high concentration of values up to 25°. The highest occurrence of very steep surfaces has been observed at –9 m depth, with high frequency of values up to 25°, and a wide distribution of steepest values up to 50°. A similar distribution and range of values characterizes the fourth level, at about –13 m depth. All the four levels present a similar trend of the slope distribution, with the steepest surfaces generally located at lowest depth. The increase of depth corresponds to wider steep areas and to the decreasing of the slope. This feature outlines a general concave morphology of the four bathymetric levels, with a very steep upper part followed by a less steep and more extended basal sector.

Convex breaks of slopes (C < $-10° m^{-1}$) are mainly located at three depth levels (Fig. 7). The shallowest and the deepest ones, respectively located at –2 to –3 m and –10 to –12 m, have a high presence of curvature values up to $-15° m^{-1}$, with maximal values up to about $-30° m^{-1}$. The most populated level is located at –6 to –7 m and has a very high occurrence of values up to $-15°m^{-1}$, and maximal values up to $-50°m^{-1}$. The bathymetrical levels with high convex surfaces are shifted towards shallower depth respect to very steep slope ones, as the breaks of slopes are generally the upper boundary of very steep slopes.

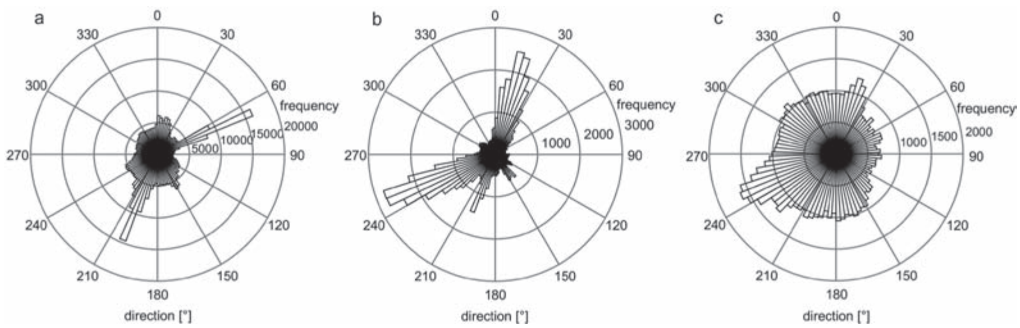

Fig. 8. Aspect of a) steep slopes (10° < S < 20°), b) very steep slopes (S > 20°) and c) very convex surfaces ($C < -14\,m^{-1}$). Radial-values indicate the number of pixels; the Azimuth-values are compass direction in degrees, with 0 = north.

Steep slopes have two main aspect directions, toward ENE and SSW. Secondary facing directions are NNE and SE (Fig. 8a). The very steep slopes are most facing toward NNE and WSW, with remaining surfaces dipping toward SSW and SE (Fig. 8b). Those directions are consistent with the orientation of convex breaks of slope, mainly facing toward NNE and WSW (Fig. 8c).

Steep slopes, very steep slopes and breaks of slope have a closed correlation in terms of orientation, mostly consistent with the general orientation of the ebb-channel slopes (NE and SW) and, to a lesser extent, of sand waves flanks (SE and NW).

4.2.2 *Sediment characterization*

The correlation of geomorphometric features and seabed composition is best carried out using backscatter intensity and sediment samples (Fig. 6). Low backscatter intensities, ranging from –60 and –45 dB, characterize the very steep slopes (Fig. 6d, e) and they are located directly deeper of the lowest values of profile curvature (Fig. 9, profiles a, b). According to collected samples, these backscatter values are given by the presence of peat layers and cohesive clay (Fig. 6g).

As well as the values of morphometric parameters, also the backscatter intensities of those steep sectors are distinct from the intermediate flat surfaces and the bottom of the deeply incised depression. Flat surfaces are characterized by quite constant slope and profile curvature and a mean backscatter intensity of –33 dB, given by sandy sediments (Fig. 9a). The bottoms of depressions have higher variability of morphometric values due to the rough morphology. Backscatter intensity is between –37 and –24 dB, with a mean value of about –32 dB (Fig. 9b). Such variability is given by the presence of mixed sediments made of sand, shells and peat fragments (Fig. 6h).

On sand waves, backscatter intensities range from –30 to –25 dB. The trend of backscatter is mainly consistent to the variation of morphometric parameters given by the medium and small sand waves morphology, with higher backscatter values on the throws and lower on the crests (Fig. 9c). On large sand waves, the backscatter intensity is quite constant, even though their morphology gives variable morphometric parameters. Samples reveal the presence of heterogeneous sediments, ranging from gravelly sand to sand, with local variations of the coarse fraction mainly made of shells and shell fragments (Fig. 6i).

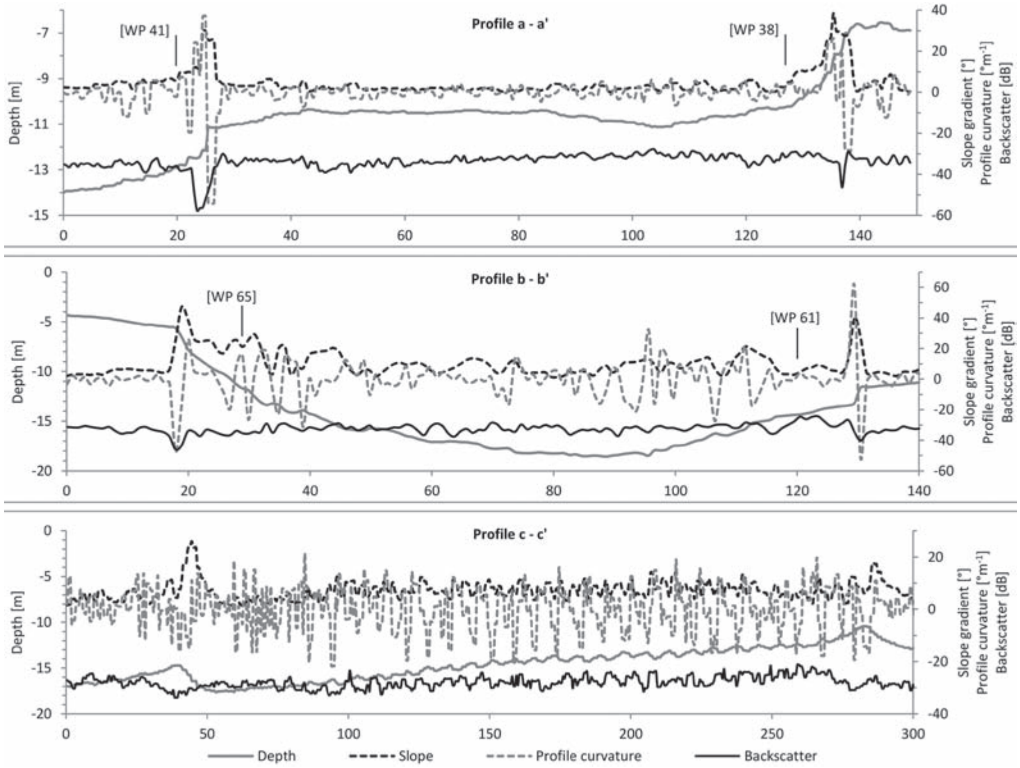

Fig. 9. Comparison of morphometric parameters and backscatter intensity. Profiles refer to Fig. 6.

5 *Discussion*

The morphology of four tidal inlets was investigated by the application of a geomorphometric approach, allowing quantitative analysis of bathymetry and providing repeatable results. The statistical analysis of morphometric parameters of four tidal inlets was possible by the availability of high-resolution data, collected by swath bathymetric systems, processed to correct spikes, artefacts and the water column effects. As geomorphometric methods are strongly conditioned by the quality of data (Pike et al. 2009), the use of a bathymetric datasets collected by the same instrument and processed with same methods, ensured the homogeneity of data quality and the quantitative comparability of the DEMs across the investigated inlets.

The large availability of homogeneous bathymetrical datasets allows classifying slope and profile curvature according to the peculiar morphology of the Wadden Sea tidal inlets. The classification outlines a general consistency of morphology over four inlets, even though a larger variability characterizes the profile curvature values. This can be due to the more noisy nature of curvature, since residual artefacts may still be present in the final DEMs (Lecourse et al. 2016). They are introduced by some technical factors typically affecting the hydroacoustic surveys, as the position accuracy and the water column effects (Lurton 2002). Moreover, the intense morphodynamics causes rapid bathymetric variations (Meyer 2014), making the inter-

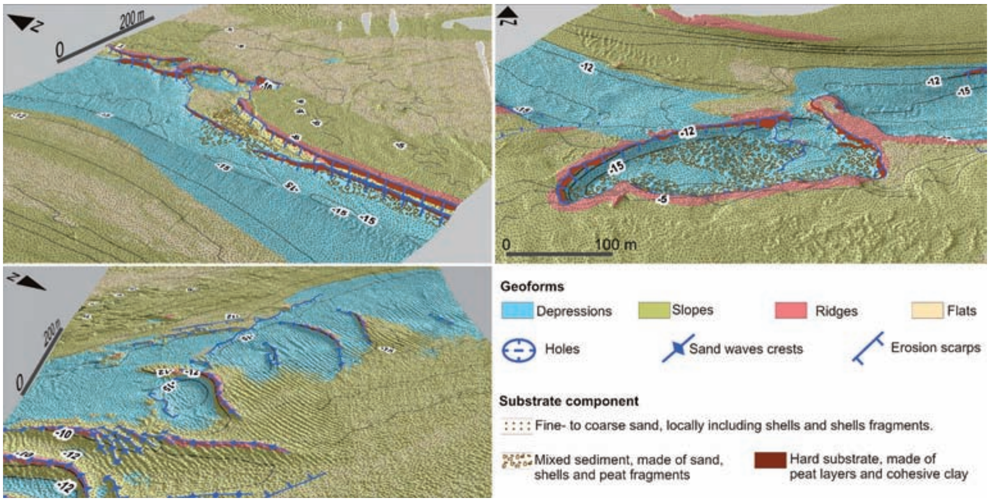

Fig. 10. Geoforms and substrate characterization, resulting from the integration of the geomorphometric analysis and backscatter intensity. Vertical exageration 3×.

polation of overlapping areas surveyed at different times problematic. The variability of profile curvature over the four inlets can also be related to local heterogeneities of substrate nature, which still need further investigations by means of backscatter and samples to be correlated to morphometric parameters.

Classified slope and profile curvature have been used for the detailed analysis of Otzumer Balje to map steep slopes and breaks of slope. The broad-scale morphological classification carried out by the BPI, identifies four morphological zones (Fig. 10) corresponding to the ebb tidal channel, the small tributary channels, the channels upper edges, as well as the crest of the large sand waves on the channels bottom (Boothroyd, 1985, Ernstsen et al., 2005).

The fine-scale BPI and morphometric parameters identify different types of minor bedforms. Respect to those proposed by Weiss 2001 and widely employed in previous marine studies (Iampietro et al. 2005, Lundbald et al. 2006, Wilson et al. 2007), the used classification criteria allow us to identify smoothed and small-scaled bedforms, including sand waves, scarps and deeply incised depressions. Even though such bedforms are characterized by the same classes of slope and profile curvatures, they return different backscatter intensities with very low values on scarps and higher values on sand waves (Fig. 9). The different backscatters on similar morphometric parameters constitutes a useful constraint to consider the backscatter mainly depending on the sediment type rather than on the morphology, and to assume a reliable processing of the received signal according with the sonar equation (Lamarche et al. 2011, Lurton 2002).

The morphometric analysis assumes a geologic and geomorphologic meaning by the comparison with processed backscatter and samples, as they give most of the contribution to characterize the substrate and differentiate unconsolidated sediments and hard-layers (Diesing et al. 2009, 2014) being optical methods, as cameras, not usable due to the water turbidity of the Wadden Sea.

As result, we were able to classify the seabed in terms of bedforms and sediment type, according to the main schemes for seabed geomorphological, ecological and biotope classification (Davies et al. 2004, Madden & Grossman 2007, Finkl et al. 2008). Very steep slopes and breaks of slopes identify three main systems of scarps, whose spatial distribution is quantitatively described by the analysis of their depth and orientation. Scarps are located along the slopes of the ebb-channel, with a main direction parallel to the channel, at three different depths at –5 m to –6 m, –8 m to –10 m and –12 m to –13 m (Fig. 10a). They are given by the alternation of sandy sediments and hard substrate layers, made of peat and very cohesive clay. Hard layers constitute the scarps bounding two deeply incised holes located on the margin of the ebb-channels, filled by mixed sediments made of sand, shells and peat fragments (Fig. 10b). The depth and litho-stratigraphical features of the hard substrate outcrops are consistent with the Holocene basal clastic sequence (Streif 1998, 2004), as deduced by the intersection of the actual bathymetry with the map of the Holocene basis and stratigraphic cores (GPDN 2009, 2013).

Sand waves are present on the channels bottom (Fig. 10). They present flanks and crest with directions generally perpendicular to those of the ebb-channel, outlined by a high occurrence of steep surfaces facing toward SE and NW and the more scattered orientation of profile curvature. Even though backscatter shows quite constant intensities and samples outline sandy sediments, slight variations of backscatter across the sand waves are present. Assuming a consistent calibration and compensation, these variations can be considered more related to a sediment sorting across the sand waves rather than to morphological effects on backscatter (Lamarche et al. 2011). This is consistent with several sedimentological investigations carried out on sand waves of the Wadden Sea by the use of systematic sampling (Ernsten et al. 2005, Svenson et al. 2009).

6 *Conclusion*

The paper proposes an objective approach to characterize the seabed, which transforms high-resolution bathymetric data, backscatter intensities and samples into meaningful geomorphological and geological information.

The morphometric analysis provides a general morphologic classification of the subtidal areas of the Wadden Sea tidal inlets, based on a substantial homogeneous high-resolution bathymetrical dataset. It gives a substantial contribution to objectively identify bedforms at broad- and local-scale, as well as to give preliminary information about substrate variations.

We focus on the importance to join the quantitative morphometric interpretations with calibrated-compensated backscatter intensities and samples, to extract acceptable information on the seabed nature. This is possible by the use of modern swath bathymetrical systems, as they simultaneously collect bathymetry and backscatter intensity. That ensures the consistency of hydro-acoustic datasets and allows an optimal processing of backscatter strength according to the sonar equation, returning suitable results for a quantitative comparison of datasets.

Compared to the traditional manual one, this approach i) reduces the operator bias and subjectivity, ensuring consistency of classification results, ii) does not require intensive computer processing power, and it decreases the time and cost of data interpretation, iii) it is mainly implemented in GIS environment, allowing further spatial and statistical analysis to be carried out. A number of sources of uncertainty may still affect the final products. Even though advances in survey and processing technologies are quite rapid, artefacts are still common in hydro-acoustic data and could affect the derivation of some morphometric parameters and backscatter intensity. This may result in misclassification coinciding with noise or gaps in the data, that could be partially improved during the data acquisition and processing.

Further investigations based on the quantitative comparison of morphometric parameters, backscatter and samples will be aimed to improve the classification of morphometric parameters for the tidal inlets systems.

In conclusion, within this integrated approach, it is possible to quantitatively analyse the complex geomorphology and substrate nature of the Wadden Sea tidal inlets. The characterization of hard substrates, unconsolidated sediments, erosive and depositional bedforms allows the implementation of most of the geological, geomorphological and biotope classification schemes, providing valuable information for multidisciplinary ecological investigations in agreement with the monitoring requirements of the European Directives.

Author Contributions

FM undertook the geomorphometric analysis, backscatter processing, sampling, samples analysis, and seabed mapping, and provided the manuscript. GB contributed to geomorphometric analysis and substantially contributed to revisions. PB, DH and RT undertook the hydro-acoustic survey and bathymetrical processing. AW supervised the research work.

References

Augustine, J. M. & Lurton, X. (2005): Image amplitude calibration and processing for seafloor mapping sonars. – Oceans 2005 – Europe **1:** 698–701.

Bartholomä, A., Holler, P., Schrottke, K. & Kubicki, A. (2011): Acoustic habitat mapping in the German Wadden Sea – Comparison of hydro-acoustic devices. – Journal of Coastal Research **64:** 1–5.

Beaudoin, J., Hughes Clarke, J. E., Van Den Ameele, E. & Gardner, J. (2002): Geometric and radiometric correction of multibeam backscatter derived from Reson 8101 systems. – Canadian Hydrographic Conference 2002, Toronto, Canada, Proceedings, CDROM.

Boothroyd, J. C. (1985): Tidal Inlets and Tidal Deltas. – In: Davis R. A. (ed.): Coastal Sedimentary Environments. – Springer-Verlag, 716 pp., New York, Berlin, Heidelberg, Tokyio.

Brown, C. J., Smith, S. J., Lawton, P. & Anderson, J. T. (2011): Benthic habitat mapping: A review of progress towards improved understanding of the spatial ecology of the seafloor using acoustic techniques. – Estuarine, Coastal and Shelf Sciences **92:** 502–520.

Bungenstock, F. & Weerts, H. J. (2010): Holocene sea-level curves for the German North sea cost. – International Journal of Earth Sciences (Geol. Rundsch.) **101:** 1083–1090.

Chang, T. S., Flemming, B. W., Tilch, E. L., Bartholomä, A. & Wöstmann, R. (2006): Late Holocene stratigraphic evolution of a back-barrier tidal basin in the East Frisian Wadden Sea, southern North Sea: transgressive deposition and its preservation potential. – Facies **52:** 329–340.

Dankers, N.,Van Duin, W., Baptist, M., Dijkman, E. & Jenny, C. (2012): The Wadden Sea in the Netherlands:Ecotopes in a World Heritage Barrier Island System. – In: Harris, P. T. & Baker, E. K. (eds.): Seafloor geomorphology as benthic habitat. – Elsevier Insights, 213–226.

Davies, C. E., Moss, D. & Hill, M. O. (2004): EUNIS Habitat Classification revised. – Report to the European Topic Centre on Nature Protection and Biodiversity, European Environment Agency, October 2004, 310 pp.

De Reu, J., Bourgeois, J., Bats, M., Zwertvaegher, A., Gelorini, V., De Smedt, P., Chu, W., Antrop, M., De Maeyer, P., Finke, P., Van Meirvenne, M., Verniers, J. & Crombé, P. (2013): Application of the topographic position index to heterogeneous landscapes. – Geomorphology **186:** 39–49.

Diesing, M., Coggan, R. & Vanstaen, K. (2009): Widespread rocky reef occurrence in the central English Channel and the implications for predictive habitat mapping. – Estuarine, Coastal and Shelf Science **83:** 647–658.

Diesing, M., Green, S. L., Stephens, D., Murray Lark, R., Stewart, H. A. & Dove, D. (2014): Mapping seabed sediments: Comparison of manual, geostatistical, object-based image analysis and machine learning approaches. – Continental Shelf Research **84:** 107–119.

Dissanayake, D. M. P. K., Wurpts, A., Miani, M., Knaack, H., Niemeyer, H. D. & Roelvink, J. A. (2012): Modelling morphodynamic response of a tidal basin to an anthropogenic effect: Ley Bay, East Frisian Wadden Sea – applying tidal forcing only and different sediment fractions. – Coastal Engineering **67:** 14–28.

Dittmann, S. (ed.) (1999): The Wadden Sea ecosystem. Stability, Properties and Mechanism. – Spinger Edition, 307 pp., Heidelberg.

Erdey-Heydorn, M. D. (2008): An ArcGIS seabed characterization toolbox developed for investigating benthic habitats. – Marine Geodesy **31:** 318–358.

Ernstsen, V. B., Noormets, R., Winter, C., Bartholomä, A., Flemming, B. W. & Bartholdy, J. (2005): Development of subaqueous barchanoid dunes due to lateral flow and grain size variability in a tidal inlet channel of the Danish Wadden Sea. – Journal of Geophysical Research **110:** F04S08, doi: 10.1029/2004JF000180.

Evans, D. A., Williard, K. W. J. & Schoonover, J. E. (2016): Comparison of terrain indices and landform classification procedures in Low-Relief agricultural fields. – Journal of Geospatial Applications in Natural Resources **1:** 17 pp, available at http://scholarworks.sfasu.edu/j_of_geospatial_applications_in_natural_resources/vol1/iss1/1.

Finkl, C. W. & Andrews, J. L. (2008): Shelf Geomorphology along the Southeast Florida Atlantic Continental Platform: Barrier Coral Reefs, Nearshore Bedrock and Morphosedimentary Features. – Journal of Coastal Research **24** (4): 823–849.

Flemming, B. W. & Davis, R. A. (1994): Holocene evolution, morphodynamics and sedimentology of the Spiekeroog Barrier Island System (Southern North Sea). – Senckenbergiana Maritima **24:** 117–155.

Fonseca, L. & Calder, B. (2006): Geocoder: An Efficient Backscatter Map Constructor. – Center for Coastal and Ocean Mapping, University of New Hampshire, Durham, NH 03824.

GPDN (2013): Holozänbasis Küste. – Geopotenzial Deutsche Nordsee – Nordsee Kartenserver, www.gpdn.de.

GPDN (2009): Bohrungen der Bohrdatenbank von Niedersachsen (BDN). – Geopotenzial Deutsche Nordsee – Nordsee Kartenserver, www.gpdn.de.

Hayes, M. O. (1980): General morphology and sediment patterns in tidal inlets. – Sedimentary Geology **26:** 139–156.

Iampietro, P. J., Kvitek, R. G. & Morris, E. (2005): Recent advances in automated genus-specific marine habitat mapping enabled by high-resolution multibeam bathymetry. – Marine Technology Society Journal **29** (3): 83–93.

Ismail, K., Huvenne, V. A. I. & Masson, D. G. (2015): Objective automated classification technique for marine landscape mapping in submarine canyons. – Marine Geology **326:** 17–32.

Jasiewicz, J., Zwoliński, Zb., Mitasova, H. & Hengel, T. (eds.) (2015): Geomorphometry for geosciences. – Adam Mickiewicz University in Poznań, Institute of Geoecology and Geoinformation, International Society of Geomorphometry, 278 pp.

Jenness, J. (2006): Topographic Position Index (tpi_jen.avx) extension for ArcView 3.x, v. 1.3a. – Jenness Enterprises, available at: http://www.jennessent.com/arcview/tpi.htm.

Jenks, G. F. & Caspall, F. C. (1971): Error on Choroplethic Maps. Definition, Measurement, Reduction. – Annals of the Association of American Geographers **61:** 217–244.

Ladage, F., Meyer, C., Stephan, H. J. & Niemeyer, H. D. (2006): Morphologische Entwicklung im Seegat Otzumer Balje und seinem Einzugsgebiet. – Dienstbereich Forschungsstelle Küste 2/2006.

Lamarche, G., Lurton, X., Verdier, A.-L. & Augustin, J.-M. (2011): Quantitative characterization of seafloor substrate and bedforms using advanced processing of multibeam backscatter. Application to the Cook Strait, New Zealand. – Continental Shelf Research **31** (2): 93–109.

Le Bas, T.P. & Huvenne, V. A. I. (2009): Acquisition and processing of backscatter data for habitat mapping – comparison of multibeam and sidescan systems. – Applied Acoustics **70:** 1248–1257.

Lecours, V., Dolan, M. F. J., Micallef, A. & Lucieer, V. (2016): A review of marine geomorphometry, the quantitative study of the seafloor. – Hydrology and Earth System Sciences **20:** 3207–3244.

Lecours, V., Lucieer, V. L., Dolan, M. F. J. & Micallef, A. (2015): An ocean of possibilities: applications and challenges of marine geomorphometry. – In: Jasiewicz, J., Zwoliński, Zb., Mitasova, H. & Hengel, T. (eds) (2015): Geomorphometry for geosciences, Adam Mickiewicz University in Poznań, Institute of Geoecology and Geoinformation. – International Society of Geomorphometry, 23–26.

Lüders, K. (1953): Die Entstehung der ostfriesischen Inseln und der Einfluß der Dünenbildung auf den geologischen Aufbau der ostfriesischen Küste. – Probleme der Küstenforschung im südlichen Nordseegebiet **5:** 5–14.

Lundbald, E. R., Wright, D. J., Miller, J., Larkin, E. M., Rinehart, R., Naar, D. F., Donahue, B. T., Anderson, S. M. & Battista, T. (2006): A benthic terrain classification scheme for American Samoa. – Marine Geodesy **29:** 89–111.

Lurton, X. (2002): An introduction to underwater acoustics. – Springer-Verlag, 347 pp., Berlin, Heidelberg.

Lurton, X. & Lamarche, G. (2015): Introduction to backscatter measurements by seafloor-mapping sonars. – In: Lurton, X. & Lamarche, G. (eds.): Backscatter measurements by seafloor mapping sonars. – Guidelines and Recommendations, 11–24, http://geohab.org/wpcontent/uploads/2014/05/BSWG-REPORT-MAY2015.pdf.

Madden, C. J. & Grossman, D. H. (2007): A framework for a coastal/marine ecological classification standard (CMECS). – In: Todd, B. J. & Greene, H. G. (eds.): Mapping the seafloor for habitat characterization. – Geological Association of Canada, Special Paper **47:** 185–209.

Meyer, C. (2014): Morphodynamische Analysen im Bereich des Norderneyer Seegats und seines Einzugsgebietes. – Niedersächsischer Landesbetrieb für Wasserwirtschaft, Küsten- und Naturschutz, Forschungsstelle Küste, Untersuchungsbericht **01:** 23 pp.

Micallef, A., Berndt, C., Masson, D. G. & Stow, D. A. V. (2007): A technique for the morphological characterization of submarine landscapes as exemplified by debris flows of the Storegga Slide. – Journal of Geophysical Research **112:** F02001.

Micallef, A., Le Bas, T. P., Huvenne, V. A. I., Blondel, P., Hühnerbach, V. & Deidun, A. (2012): A multi-method approach for benthic habitat mapping of shallow coastal areas with high-resolution multibeam data. – Continental Shelf Research **39–40:** 14–26.

Miccadei, E., Mascioli, F., Orrù, P. E. & Puliga, G. (2011): Late Quaternary paleolandscape of submerged inner continental shelf areas of Tremiti Islands archipelago (northern Puglia). – Geografia Fisica e Dinamica Quaternaria **34/2:** 223–234.

Miccadei, E., Orrù, P. E., Piacentini, T., Mascioli, F. & Puliga, G. (2012): Geomorphological map of Tremiti Islands Archipelago, Puglia, Southern Adriatic Sea, Italy, scale 1 : 15,000. – Journal of Maps **8/1:** 74–87.

Pike, R. J., Evans, I. S. & Hengl, T. (2009): Geomorphometry: a brief guide. – Development in Soil Science **33:** 3–30.

Ragutzki, G. (1982): Verteilung der Oberflächensedimente auf den niedersächsischen Watten. – Jahresbericht 1980, Forschungsstelle für Insel und Küstenschutz **32:** 55–68.

Son, C. S., Flemming, B. W. & Bartholomä, A. (2011): Evidence for sediment recirculation on an ebb-tidal delta of the East Frisian barrier-island system, southern North Sea. – Geo-Marine Letters **31:** 87–100.

Streif, H. (1998): Die Geologische Küstenkarte von Niedersachsen 1 : 25.000 – eine neue Planungsgrundlage für die Küstenregion. – Zeitschrift für angewandte Geologie **44:** 183–194.

Streif, H. (2004): Sedimentary record of Pleistocene and Holocene marine inundations along the North Sea coast of Lower Saxony, Germany. – Quaternary International **112:** 3–28.

Svenson, C., Ernsten, V. B., Winter, C., Bartholomä, A. & Hebbeln, D. (2009): Tide-driven sediment variations on a large compound dune in the Jade tidal inlet channel, Southeastern North Sea. – Journal of Coastal Research **56:** 361–365.

Wang, Z. B., Hoekstra, P., Burchard, H., Ridderinkof, H., De Swart, H. E. & Stive, M. J. F. (2012): Morphodynamics of the Wadden Sea and its barrier island system. – Ocean and Coastal Management **68:** 39–57.

Weiss, A. (2001): Topographic Position and Landforms Analysis. – Poster presentation, ESRI User Conference, San Diego, CA.

Wilson, M. F. J., O'Connell, B., Brown, C., Guinan, J. C. & Grehan, A. J. (2007): Multiscale terrain analysis of multibeam bathymetry data for habitat mapping on the continental slope. – Marine Geodesy **30:** 3–35.

Zeiler, M., Schulz-Ohlberg, J. & Figge, K. (2000): Mobile sand deposits and shoreface sediment dynamics in the inner German Bight (North Sea). – Marine Geology **170:** 363–380.

Zeiler, M., Schwarzer, K. & Ricklefs, K. (2008): Seabed morphology and sediment dynamics. – Die Küste **74:** 31–44.

Address of the authors:

Coastal Research Station, Lower Saxony Water Management, Coastal Defence and Nature Conservation Agency, An der Mühle 5, 26548 Norderney, Germany,
e-mail: francesco.mascioli@nlwkn-ny.niedersachsen.de

Manuscript received: 29 February 2016
Revision required: 11 January 2017
Revised version received: 4 March 2017
Accepted: 7 March 2017